A Study of Thin Foil Explosion

Tatiana A. Shelkovenko, Sergey A. Pikuz, Ivan N. Tilikin, Vera M. Romanova, Sergey N. Mishin, Levon Atoyan, and David A. Hammer, *Member, IEEE*

***Abstract*— The explosion of thin flat and cylindrical foils has been studied on the BIN (270 kA, 100-ns rise time), XP (500 kA, 100-ns rise time), and COBRA (1.0 MA, 100-ns rise time) pulsed-power generators. On all three generators, hybrid and standard 4-wire X-pinches were used to provide soft X-ray radiography with better than 3-μm spatial resolution and 1-ns temporal resolution. This enabled a detailed exploration of the dependence of the exploded structure of the foil on its initial structure and the current density flowing through it. With sufficient current density in the foils, bubbles were observed to form in the center of the foils; the higher the current density, the larger is the bubble diameters.**

***Index Terms*— Flat foil, foil explosion, liner, plasma pinch, X-ray imaging.**

I. Introduction

FOR more than 60 years, many laboratories have been studying the electrical explosion of metal loads under high current densities [1]–[12]. During the last two decades, a major area of study has been the nanosecond explosion of single fine wires [2]–[5], and wire arrays of various configurations [6]–[11]. This was due to the progress in the creation of powerful sources of soft X-ray radiation based on multiwire assemblies on the Z generator [8]–[11], including for use in inertial confinement fusion research [10], [11]. During the past few years, the Z generator has addressed a magnetized liner inertial fusion for the fusion research involving a gas-filled cylindrical liner made of aluminum or beryllium placed in an external magnetic field and with initial heating of the gas by a powerful laser [12], [13].

Medium size generators at universities, such as COBRA [14] at Cornell University, ZEBRA [15] at the University of Nevada, Reno, and MAIZE [16] at the University of Michigan, have been used recently to study instability formation in thin cylindrical liners. In addition, studies of flat foil explosions can help to understand the formation of small-scale instabilities in the liners [17], [18]. For studies involving thin flat foils, it is possible to use small generators with currents from 10 to 500 kA [17]–[20]. For example, the small generator wire explosion generator (8 kA, 20 kV, 500 ns) at the Institute of High Current Electronics (Tomsk, Russia) [18]–[20] has been used. Flat foils are also used for applications such as shock wave generation [21], the creation of fast switches for powerful generators [22], and the interaction of XUV radiation with thin flat foils [23]. The structure of the foils before the explosion and its influence on the explosion of the foil was not taken into account. In this paper, the important role of the original structure of the foil on the formation of instabilities in the exploded foil is shown.

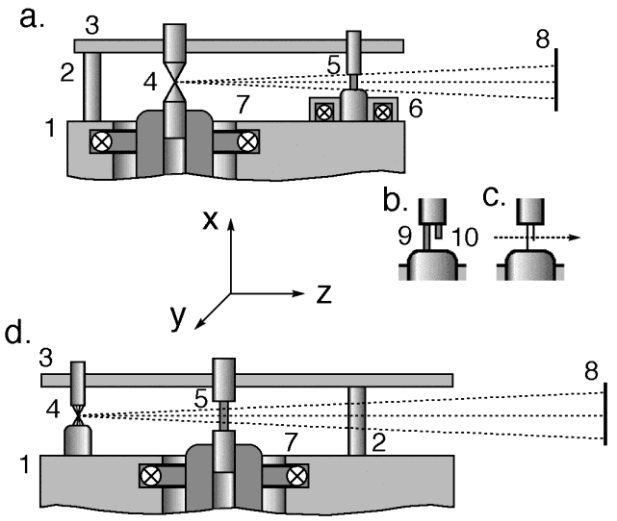

Fig. 1. Schematic of X-ray backlighter imaging on (a) BIN and XP generators and (d) COBRA generator. Diagrams of the return current circuit load on the BIN and XP generators (b) view on the load with the y-direction (c) on the z-direction. 1: ground electrode, 2: return current rod, 3: high voltage electrode, 4: HXP or standard X-pinch, 5: investigated load, 6 and 7: Rogowski coils, 8: film, 9: exploding foil, and 10: disconnected (unexploded) foil.

II. Experimental Setup

Basic experimental setups are presented in Fig. 1. Images of dense cores were obtained using high-resolution X-ray point-projection radiography with standard or hybrid X-pinches (HXPs) as sources of probing radiation. Experiments were performed on pulsers with the output current from 250 kA to 1.2 MA with rise times about 100 ns (see Table I). In all cases, the X-pinch X-ray burst is in subnanoseconds, and

Manuscript received December 17, 2017; revised April 4, 2018 and May 21, 2018; accepted May 22, 2018. This work was supported in part by the National Nuclear Security Administration Stewardship Sciences Academic Programs through the Department of Energy under Grant DE-NA0003764 and in part by the Russian Fund for Basic Research under Grant 18-08-00631. The review of this paper was arranged by Senior Editor F. Beg. *(Corresponding author: Sergey A. Pikuz.)*

T. A. Shelkovenko, S. A. Pikuz, L. Atoyan, and D. A. Hammer are with the Laboratory of Plasma Studies, Cornell University, Ithaca, NY 14850 USA (e-mail: taniashel@yahoo.com; pikuz@yahoo.com; levo.ato@gmail.com; dah5@cornell.edu).

I. N. Tilikin, V. M. Romanova, and S. N. Mishin are with the P. N. Lebedev Physical Institute, Russian Academy of Sciences, Moscow 119991, Russia (e-mail: ivan.tilikin@gmail.com; vmr@inbox.ru; mishin@mail.ru).

Color versions of one or more of the figures in this paper are available online at http://ieeexplore.ieee.org.

Digital Object Identifier 10.1109/TPS.2018.2852063

TABLE I
GENERATORS, FOILS, AND SOURCE OF RADIATION USED IN EXPERIMENTS

Generators	Load	Current kA	Source
XP (450 kA, 100-150 ns) Cornell University	Foil Al, Cu, Ti, Ni, 16 μm x 2-5 mm	60 - 250	HXP Mo,Ag 50μm (Fig.1a)
COBRA (1 MA, 100-200 ns) Cornell University	Foil Al, Cu, Ti, Ni, Ta 4-16μm x 5-10mm Liner 4-16μm x 4mm	1000	SXP Mo 4x25 μm (Fig.1b)
BIN (250 kA, 100-150 ns) P.N.Lebedev Institute,	Foil Al, Cu, Ni 1-16μm x 0.3-5mm	40 - 70	HXP Mo 30μm (Fig.1a)

so the image is essentially instantaneous in the time scale of expansion of the exploding foils [24]. Two approaches in different forms have been used to drive current through exploding foil loads for these experiments. Simplified schematic of the various arrangements is shown in Fig. 1(a)–(d).

Three generators with the parameters given in Table I were used in the experiments presented in this paper. Point-projection radiography of the exploded and unexploded foils was the main diagnostics used in the experiments. On the BIN and XP generators, the source of backlighting radiation was an HXP placed as the main load of the generators [Fig. 1(a)]. The foils were placed in the return current circuit in one of the two return current posts [Fig. 1(a)–(c)]. To change the current through the foil, the geometry of the HXP, the rod, and the foil were changed to adjust the inductance of the circuits. The currents through the HXP and the foil were measured using calibrated Rogowski coils. On the COBRA generator, the exploded foil was placed in the main circuit while the HXP was in the return current circuit [Fig. 1(d)]. Unexploded foils on the COBRA were placed at a different angle to the HXPs and were studied as test objects.

The geometry of the experiments and the size of the radiation source from the HXP or the 4-wire X-pinch can provide a spatial resolution better than 3 μm [24]. The time resolution of the point-projection radiography with the X-pinch as a source of radiation is better than 0.1 ns [24].

All information about the generator parameters, foils, and X-pinches are presented in Table I. Currents through the foils and voltages were measured on all generators, but the electrical circuits were too complicated to correctly subtract the inductive component of the voltage. Thus, we currently cannot carry out calculations of the energy deposited in the exploded foils. Diamond photoconducting detectors (PCDs) with different filters were used to detect the X-pinch burst intensity and timing. Currents and X-pinch X-ray signals measured on the XP and BIN generators are shown in Fig. 2.

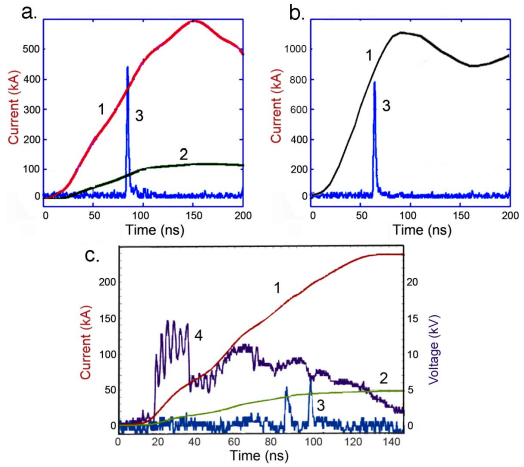

Fig. 2. (a) XP, (b) COBRA, and (c) BIN generator signals. 1: generator current, 2: current through the foils, 3: PCD signals recording X-pinch X-ray bursts of X-ray energy higher than 1.2 keV (the HXP presented in Fig. 2(c) developed two hot spots and radiated two X-ray bursts [17]), and 4: voltage on the foil measured on the BIN generator.

TABLE II
INITIAL STRUCTURE OF THE FOILS USED IN THE EXPERIMENTS

#	Material	Thickness, μm	Initial structure
1	Al	4	No significant structure
2	Al	11	No significant structure
3	Al	16	1-d structure with ~30 μm period
4	Ti	12.5	2-d structure with 20-40 μm period
5	Ni	5	No visible structure
6	Ni	7	No visible structure
7	Cu	1	No visible structure
8	Cu	7	1-d structure with variable period
9	Cu	10	1-d structure with ~10 μm period

III. EXPERIMENTAL RESULTS

While executing the experiments presented herein, we found that some of the foils had a well-defined initial structure in one direction, while other foils did not appear to have any visible initial structure (at least to within observable limits [24]). In the case of very thin and low Z foils (4-μm Al or 1-μm Cu foils), the contrast of the point-projection radiography method was insufficient to see the foil structure. In Table II, all foils used in the experiments are characterized.

Figs. 3(a) and 4(a) present the radiographs of unexploded and exploded 16-μm-thick Al foils, respectively. To analyze the structure in the radiographs of both the unexploded and exploded foils more obvious, Fourier analysis was used for radiograph images of unexploded and exploded foils. Radiographs of exploded foils were analyzed during the early time period from the experiment's initial conditions up to the time of bubble formation [17]. The duration of this period mostly depends on the current density through the foils and the foil materials. The purpose of this procedure is the spatial filtering of the image. Fast Fourier transform (FFT) procedure of the images has been done in the beginning using ImageJ software [25]. Then, the central parts of the Fourier spectra were subjected to the inverse FFT (IFFT), filtering out high

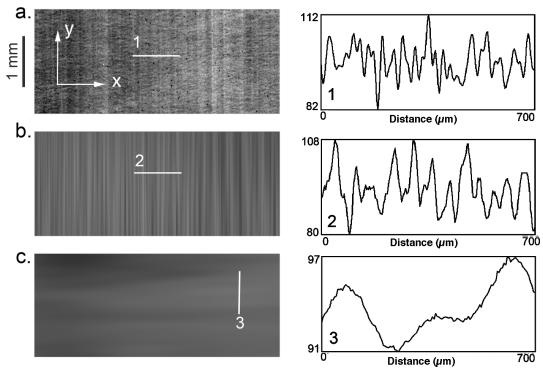

Fig. 3. (a) Radiographs of unexploded (disconnected Al foil 16 μm thick obtained on XP generator in the *xy* plane). IFFT image in (b) *y*- and (c) *x*-directions. 1–3: intensity profiles made in places shown with white lines.

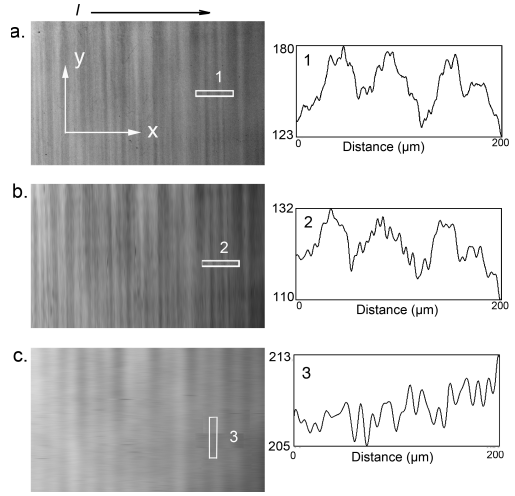

Fig. 4. (a) Radiograph image (in the *xy* plane) of exploded Al foil 16 μm thick and 2.7 mm wide ($t = 80$ ns, $I = 80$ kA, and $j = 1.85 \times 10^8$ kA/cm^2) with an initial structure perpendicular to the current obtained on XP generator in radiation of HXP with 50-μm-diameter Ag wire. (b) IFFT image in perpendicular (*y*-direction) and (c) parallel (*x*-direction) directions of the current. 1–3: intensity profiles made from the images at the places shown with white boxes. Arrow: current direction. Shot #XP7672.

spatial frequencies of the image and removing the random disturbance. We have analyzed only the main part of the foil. The edges of the foil require a more complex analysis. The filtering was performed separately in the *x*- and *y*- directions as shown in these figures.

The initial structure of the unexploded 16-μm Al foil [Fig. 3(a), intensity profile 1] is about 30-μm scale. The IFFT also shows a structure with about 30-μm scale in one direction. In the other direction, the structure was not observed. The explosion of the same foil on the BIN and XP generators showed a very similar structure in one direction with about 60-μm scale. In Fig. 4, the result of the foil explosion on the XP generator is shown. In this example, the initial structure of the foil was perpendicular to the current through the foil. Note that a similar scale structure of the exploded 16-μm Al foil was recorded on all three generators at different times with different currents but at nearly the same current density at the moment of the imaging. A similar structure was also recorded in the case of cylindrical liner made from this foil exploded on the COBRA generator [Fig. 5(a)].

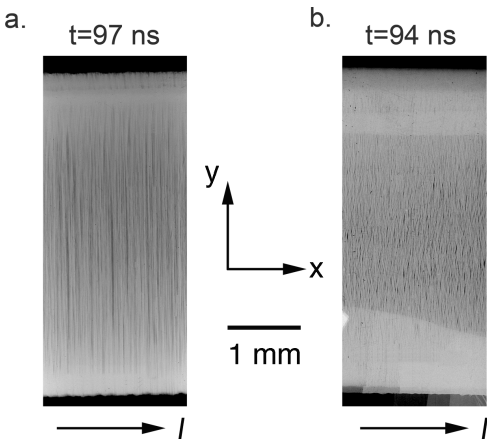

Fig. 5. (a) and (b) Radiographs of exploded Al liner (16-μm Al foil, 4 mm diameter, $j = 4.0 \times 10^8$ kA/cm^2) obtained on the COBRA generator in the *xy* plane using arrangement 1d. Initial structure of the foil was perpendicular (*y*-direction) to the current in (a) and parallel (*x*-direction) to the current in (b). Arrows: current direction. Fig. 1(a)—shot #C4203. Fig. 1(b)—shot #C4205.

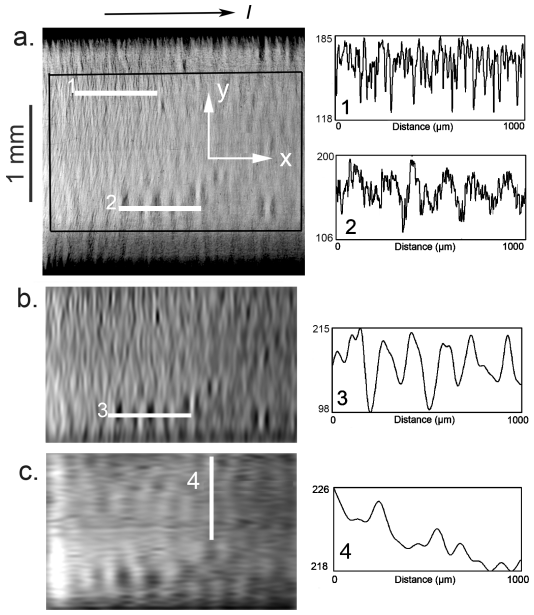

Fig. 6. (a) Radiograph image (in the *xy* plane) of exploded 16-μm-thick and 1.5-mm-wide Al foil ($t = 88$ ns, $I = 96$ kA, and $j = 4 \times 10^8$ kA/cm^2) with an initial structure parallel to the current obtained on the XP generator in radiation of HXP with a 50-μm-diameter Ag wire using the arrangement shown in Fig. 1(a). (b) IFFT image in parallel (*x*-direction) and (c) perpendicular (*y*-direction) directions of the current. 1–4: intensity profiles of the images shown with white lines. Arrow: current direction. Shot #XP7678.

When the initial structure of the foil is parallel to the current through the foil, the structure of the exploded foil is much more complicated (Fig. 6). The radiograph shows the superposition of three structures with different scales. In Table III, the scales of all developed features are presented. Small structure with about 20-μm scale is seen on the entire surface of the foil. Features with about 60- and 170-μm scales are seen in different parts of the foil surface.

From the results with foil structure parallel to the current, it is possible to say that without visible initial foil structure some instabilities develop perpendicular to the current direction. These instabilities are not so pronounced as instabilities

TABLE III

SCALES OF ALL DEVELOPED FEATURES OF THE EXPLODED FOIL FROM FIG. 6

Pulse 7678, Al foil 16 μm thickness, 1.5 mm width	Structure scale, μm
Radiograph image	~20, 60, 170
IFFT image perpendicular	~70
IFFT image parallel	No structure

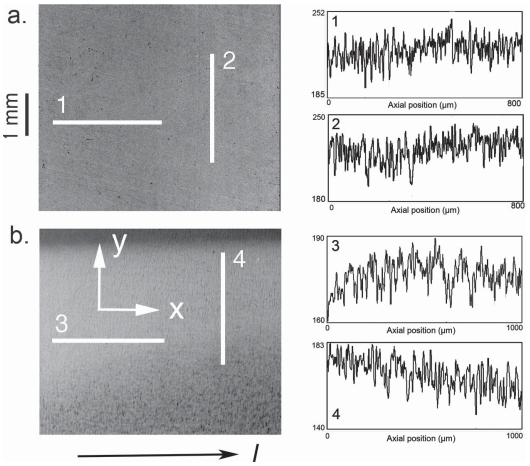

Fig. 7. (a) Radiographs of unexploded 7-μm-thick and 5-mm-wide Ni foil without pronounced initial structure and (b) exploded foil ($t = 65$ ns, $I = 730$ kA, and $j = 20, 8 \times 10^8$ kA/cm^2) obtained in the xy plane on the COBRA generator in the radiation of a 4 × 25-μm Mo X-pinch using the arrangement shown in Fig. 1(d). 1–4: intensity profiles of the images shown with white lines. Arrow on (b) shows the current direction. Shot #C4661.

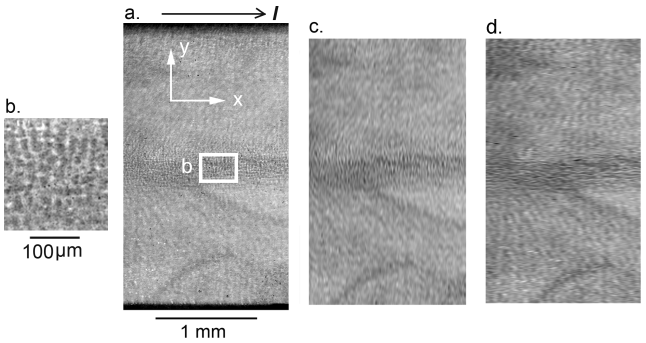

Fig. 8. (a) Radiograph of exploded 4-μm-thick and 2-mm-wide Al foil ($t = 82$ ns, $I = 94$ kA, and $j = 11.7 \times 10^8$ kA/cm^2) without visible initial structure obtained on the XP generator in radiation of an HXP with a 50-μm-diameter Ag wire using the arrangement shown in Fig. 1(a) in the xy plane. (b) Magnified image shown in Fig. 1(a) in the white rectangles. IFFT images in (c) perpendicular (y-direction) and (d) parallel (x-direction) directions of the current. Arrow: current direction. Shot #XP7717.

parallel to the current [compare intensity profiles 3 and 4 in Fig. 6].

Experiments with foils without visible initial structure have also been carried out.

Figs. 7–9 show the foils exploded under different conditions on different generators. All these foils do not have visible initial structure. In Fig. 7(a), a radiograph of an unexploded

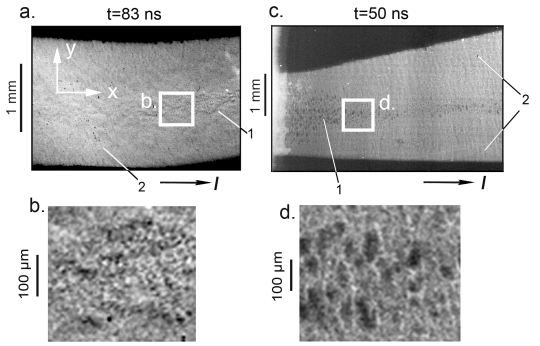

Fig. 9. (a) Radiograph images (in the xy plane) of an exploded 5-μm-thick and 1.8-mm-wide Ni foil (66 kA, $dI/dt = 9.2 \times 10^8$ A/cm^2) and (c) 1-μm-thick Cu ($I = 52$ kA, 26.6×10^8, and 32.5×10^8 A/cm^2 with left and right sides) foil that tapers from 1.6 to 2.3 mm width obtained on the BIN generator in radiation from an HXP with a 25-μm Mo wire using the experimental arrangement shown in Fig. 1(a). 1: bubbles and 2: foil core. (b) and (d) Magnified images shown in Fig. 9(a) and (c) in the white rectangles. Arrows: current direction. Fig. 1(a)—shot #B160510. Fig. 1(c)—shot #B160623.

7-μm Ni foil is shown. One can see that the foil has 6–7-μm scale structure in two directions. The IFFT of the image in Fig. 8 shows that the 4-μm-thick exploded Al foil has similar structure both parallel and perpendicular to the current direction. Fig. 9 shows almost the same structure in both directions for Ni and Cu foils exploded on the BIN generator. We can conclude that in the absence of visible structures before the explosion, the exploded foil for a long time (up to the foil boiling) also does not have a visible structure in any direction.

Only the central parts of the foils in Figs. 8 and 9 have a structure that differs from all other parts of the foils. Small growing bubbles are developed in the central parts of the foils. The bubbles are hardly seen on the exploded Ni foil in Fig. 9(a) and (b), because the foil is too thick and the current density is less than that in the case of 1-μm-thick Cu in Fig. 9(c) and (d). The current densities are 9.2×10^8 A/cm^2 for the Ni foil and (22.6–32.5) $\times 10^8$ A/cm^2 for the Cu foil. The bubble diameters are less than 10 μm in the case of 5-μm Ni foil and 40–80 μm in the case of 1-μm Cu foil. The current density in the exploded 4-μm Al foil (Fig. 8) is 11.6×10^8 A/cm^2 and the bubble diameters are about 20 μm. We can conclude that when the bubbles have appeared, the liquid foil core begins to boil.

IV. CONCLUSION

The experiments and analysis show that the core structure in exploding foils is strongly dependent on the presence of significant initial structure in the foils and the current direction relative to the initial structure up to the boiling stage of the foils. Boiling begins in the center and depends on the current density—the higher the current density, the larger is the bubble diameters. The experiments have shown that the electrothermal instability cannot be a universal explanation for the exploding foil structure.

REFERENCES

[1] W. G. Chase and H. K. Moore, *Exploding Wires*, vol. 2. New York, NY, USA: Plenum Press, 1962.

[2] D. B. Sinars *et al.*, "Experiments measuring the initial energy deposition, expansion rates and morphology of exploding wires with about 1 kA/wire," *Phys. Plasmas*, vol. 8, no. 1, pp. 216–230, 2001.
[3] S. I. Tkachenko *et al.*, "Analysis of the discharge channel structure upon nanosecond electrical explosion of wires," *Phys. Plasmas*, vol. 14, no. 12, p. 123502, 2007.
[4] A. G. Rousskikh *et al.*, "Study of the strata formation during the explosion of a wire in vacuum," *Phys. Plasmas*, vol. 15, no. 10, p. 102706, 2008.
[5] V. M. Romanova, G. V. Ivanenkov, A. R. Mingaleev, A. E. Ter-Oganesyan, T. A. Shelkovenko, and S. A. Pikuz, "Electric explosion of fine wires: Three groups of materials," *Plasma Phys. Rep.*, vol. 41, no. 8, pp. 617–636, 2015.
[6] S. V. Lebedev *et al.*, "Effect of discrete wires on the implosion dynamics of wire array Z pinches," *Phys. Plasmas*, vol. 8, no. 8, pp. 3734–3747, 2001.
[7] V. V. Aleksandrov *et al.* "Experimental and numerical studies of plasma production in the initial stage of implosion of a cylindrical wire array," *Plasma Phys. Rep.*, vol. 29, no. 12, pp. 1034–1040, 2003.
[8] J. Wu *et al.*, "X-pinch radiography for the radiation suppressed tungsten and aluminum planar wire array," *Phys. Plasmas*, vol. 19, no. 2, p. 022702, 2012.
[9] T. W. L. Sanford, "Wire number breakthrough for high-power annular z pinches and some characteristics at high wire number," *Laser Particle Beams*, vol. 19, no. 4, pp. 541–556, 2001.
[10] M. E. Cuneo *et al.*, "Compact single and nested tungsten-wire-array dynamics at 14–19 MA and applications to inertial confinement fusion," *Phys. Plasmas*, vol. 13, no. 5, p. 056318, 2006.
[11] M. E. Cuneo *et al.*, "Characteristics and scaling of tungsten-wire-array z-pinch implosion dynamics at 20 MA," *Phys. Rev. E, Stat. Phys. Plasmas Fluids Relat. Interdiscip. Top.*, vol. 71, p. 046406, Apr. 2005.
[12] S. A. Slutz *et al.*, "Scaling magnetized liner inertial fusion on Z and future pulsed-power accelerators," *Phys. Plasmas*, vol. 23, no. 2, p. 022702, 2016.
[13] R. D. McBride *et al.*, "Penetrating radiography of imploding and stagnating beryllium liners on the z accelerator," *Phys. Rev. Let.*, vol. 109, no. 13, p. 135004, 2012.
[14] L. Atoyan *et al.*, "Helical plasma striations in liners in the presence of an external axial magnetic field," *Phys. Plasmas*, vol. 23, no. 1, p. 022708, 2016.
[15] V. L. Kantsyrev *et al.*, "Radiation sources with planar wire arrays and planar foils for inertial confinement fusion and high energy density physics research," *Phys. Plasmas*, vol. 21, no. 3, p. 031204, 2014.
[16] D. A. Yager-Elorriaga *et al.*, "Discrete helical modes in imploding and exploding cylindrical, magnetized liners," *Phys. Plasmas*, vol. 23, p. 124502, 2016.
[17] T. A. Shelkovenko, S. A. Pikuz, I. N. Tilikin, A. R. Mingaleev, L. Atoyan, and D. A. Hammer, "Study of electric explosion of flat micron-thick foils at current densities of (5–50)$\times$108 A/cm^2," *Plasma Phys. Rep.*, vol. 44, no. 2, pp. 236–244, 2018.
[18] L. Atoyan *et al.*, "Technique for insulated and non-insulated metal liner X-pinch radiography on a 1 MA pulsed power machine," *Rev. Sci. Instrm.*, vol. 88, no. 11, p. 113502, 2017.
[19] V. V. Kuznetsov, V. I. Oreshkin, A. S. Zhigalin, I. A. Kozulin, S. A. Chaikovsky, and A. G. Rousskikh, "Metastable states and their disintegration at pulse liquid heating and electrical explosion of conductors," *J. Eng. Thermophys.*, vol. 20, no. 3, pp. 240–248, 2011.
[20] R. B. Baksht, A. G. Rousskikh, A. S. Zhigalin, V. I. Oreshkin, and A. P. Artyomov, "Stratification in Al and Cu foils exploded in vacuum," *Phys. Plasmas*, vol. 22, no. 10, p. 103521, 2015.
[21] M. Takayuki, N. Matsuo, M. Otsuka, and S. Itoh, "Study on metal foil explosion using high current," *Proc. SPIE*, vol. 7522, pp. 75222A-1–75222A-75222A7, Apr. 2010.
[22] V. S. Sedoi, G. A. Mesyats, V. I. Oreshkin, V. V. Valevich, and L. I. Chemezova, "The current density and the specific energy input in fast electrical explosion," *IEEE Trans. Plasma Sci.*, vol. 27, no. 4, pp. 845–850, Aug. 1999.
[23] K. N. Mitrofanov *et al.*, "Study of the expansion dynamics of the plasma of a thin aluminum foil under the action of soft X-ray emission," *Plasma Phys. Rep.*, vol. 43, no. 4, pp. 444–457, 2017.
[24] T. A. Shelkovenko, S. A. Pikuz, and D. A. Hammer, "A review of projection radiography of plasma and biological objects in X-pinch radiation," *Plasma Phys. Rep.*, vol. 42, no. 3, pp. 26–226, 2016.
[25] *Image Processing and Analysis in Java*. [Online]. Available: https://imagej.nih.gov/ij/

Authors' photographs and biographies not available at the time of publication.